Note that the three basis vectors in (5) and (6) are linearly independent for all $\boldsymbol{q}$.

A task velocity vector $\dot{\boldsymbol{r}}$ that belongs to the subspace in (5) and an associated joint velocity $\dot{\boldsymbol{q}}$ that realizes it are given by

$$\dot{\boldsymbol{r}}_1 = \begin{pmatrix} 1 \\ 0 \\ 0 \end{pmatrix} \in \mathcal{R}\left\{\boldsymbol{J}(\boldsymbol{q}_s)\right\} \qquad \Rightarrow \qquad \dot{\boldsymbol{q}}_1 = \boldsymbol{J}^{\#}(\boldsymbol{q}_s)\dot{\boldsymbol{r}}_1 = \frac{1}{L^2+2}\begin{pmatrix} 2 \\ -L \\ L \end{pmatrix},$$

where the minimum norm solution was obtained by using the pseudoinverse of $\boldsymbol{J}(\boldsymbol{q}_s)$. Indeed, it is easy to verify that $\boldsymbol{J}(\boldsymbol{q}_s)\dot{\boldsymbol{q}}_1 = \dot{\boldsymbol{r}}_1$. We provide also a second example where, for simplicity, a numerical value is specified also for q_3. Choose, e.g., $\boldsymbol{q}_{ss} = (*, \pi/2, -\pi/2)$. Then

$$\boldsymbol{J}(\boldsymbol{q}_{ss}) = \begin{pmatrix} 1 & -L & 0 \\ 0 & L & L \\ 0 & 1 & 1 \end{pmatrix}, \qquad \operatorname{rank}\left\{\boldsymbol{J}(\boldsymbol{q}_{ss})\right\} = 2, \tag{7}$$

and

$$\dot{\boldsymbol{r}}_{11} = \alpha \begin{pmatrix} 0 \\ L \\ 1 \end{pmatrix} \in \mathcal{R}\left\{\boldsymbol{J}(\boldsymbol{q}_{ss})\right\}, \ \forall\alpha \qquad \Rightarrow \qquad \dot{\boldsymbol{q}}_{11} = \boldsymbol{J}^{\#}(\boldsymbol{q}_{ss})\dot{\boldsymbol{r}}_{11} = \frac{\alpha}{L^2+2}\begin{pmatrix} L \\ 1 \\ L^2+1 \end{pmatrix}.$$

Again, $\boldsymbol{J}(\boldsymbol{q}_{ss})\dot{\boldsymbol{q}}_{11} = \dot{\boldsymbol{r}}_{11}$. On the other hand, a task velocity $\dot{\boldsymbol{r}}$ that is always unfeasible in the configuration $\boldsymbol{q}_{ss}$ is given by

$$\dot{\boldsymbol{r}}_2 = \begin{pmatrix} 1 \\ 0 \\ 1 \end{pmatrix} \notin \mathcal{R}\left\{\boldsymbol{J}(\boldsymbol{q}_{ss})\right\}.$$

In this case, the minimum norm solution given by the pseudoinverse of $\boldsymbol{J}(\boldsymbol{q}_{ss})$,

$$\dot{\boldsymbol{q}}_2 = \boldsymbol{J}^{\#}(\boldsymbol{q}_{ss})\dot{\boldsymbol{r}}_2 = \begin{pmatrix} \dfrac{2L^2+L+2}{L^4+3L^2+2} \\ -\dfrac{L^3+L-1}{L^4+3L^2+2} \\ \dfrac{L+1}{L^2+2} \end{pmatrix},$$

does never return the original task vector:

$$\boldsymbol{J}(\boldsymbol{q}_{ss})\dot{\boldsymbol{q}}_2 = \frac{1}{L^2+1}\begin{pmatrix} 1 \\ L \\ 1 \end{pmatrix} \neq \dot{\boldsymbol{r}}_2.$$

As another example, consider the task velocity

$$\dot{\boldsymbol{r}}_{22} = \begin{pmatrix} 0 \\ 1 \\ 1 \end{pmatrix} \notin \mathcal{R}\left\{\boldsymbol{J}(\boldsymbol{q}_{ss})\right\}, \quad \text{if } L \neq 1.$$

This velocity vector is also unfeasible at $\boldsymbol{q}_{ss}$, unless the link lengths are unitary ($L = 1$). In fact,

$$\dot{\boldsymbol{q}}_{22} = \boldsymbol{J}^{\#}(\boldsymbol{q}_{ss})\dot{\boldsymbol{r}}_{22} = \begin{pmatrix} \dfrac{L(L+1)}{L^4+3L^2+2} \\ -\dfrac{L+1}{L^4+3L^2+2} \\ \dfrac{L+1}{L^2+2} \end{pmatrix} \quad \Rightarrow \quad \boldsymbol{J}(\boldsymbol{q}_{ss})\dot{\boldsymbol{q}}_{22} = \frac{1}{L^2+1}\begin{pmatrix} 0 \\ L(L+1) \\ L+1 \end{pmatrix} = \dot{\boldsymbol{r}}_2|_{L=1}.$$

Finally, a generalized task force $\boldsymbol{F} = (F_x, F_y, M_z)$ that is statically balanced by $\boldsymbol{\tau} = \boldsymbol{0}$ at the joint level belongs to the null space of $\boldsymbol{J}^T(\boldsymbol{q}_s)$ (or of $\boldsymbol{J}^T(\boldsymbol{q}_{ss})$, if we assign also a numerical value to q_3). From (6), we have

$$\boldsymbol{F}_0 = \gamma \begin{pmatrix} 0 \\ 1 \\ L\sin q_3 \end{pmatrix} \in \mathcal{N}\left\{\boldsymbol{J}^T(\boldsymbol{q}_s)\right\}, \ \forall\gamma \qquad \Rightarrow \qquad \boldsymbol{\tau} = \boldsymbol{J}^T(\boldsymbol{q}_s)\boldsymbol{F}_0 = \boldsymbol{0}.$$

In fact, for a generic q_3, the momentum $M_z = L\sin q_3$ applied to the last robot link is balanced at joint 3 by the torque produced there by the force $F_y = 1$ applied at the tip, resulting in $\tau_3 = 0$[1]. Moreover, the force F_y produces no torque τ_2 at joint 2, since the second link is vertical, and no force τ_1 at joint 1, being orthogonal to it.

Consider next the inverse kinematics problem for the PRR robot when performing the specified three-dimensional task. Given a desired $\boldsymbol{r} = \boldsymbol{r}_d = (p_{xd}, p_{yd}, \alpha_d)$, we set in (1)

$$q_2 + q_3 = \alpha_d. \tag{8}$$

By reorganizing, squaring and summing the first two equations in (1), we obtain

$$(p_{xd} - q_1 - L\cos\alpha_d)^2 + (p_{yd} - L\sin\alpha_d)^2 = (L\cos q_2)^2 + (L\sin q_2)^2 = L^2.$$

Expanding the left-hand side and simplifying, we get a second order polynomial equation in q_1:

$$q_1^2 - 2\left(p_{xd} - L\cos\alpha_d\right)q_1 + \left(p_{xd}^2 + p_{yd}^2 - 2L\left(p_{xd}\cos\alpha_d + p_{yd}\sin\alpha_d\right)\right) = 0.$$

The two solutions of this equation are

$$q_{1d} = p_{xd} - L\cos\alpha_d \pm \sqrt{L^2\cos^2\alpha_d + 2L\sin\alpha_d\, p_{yd} - p_{yd}^2}. \tag{9}$$

Indeed, a (real) solution q_{1d} exists if and only if the argument of the square root in (9) is non-negative. This argument vanishes for $p_{yd} = L\sin\alpha_d \pm L$ (i.e., the two solutions of a second, auxiliary quadratic equation in p_{yd}) and is (strictly) positive for

$$p_{yd} \in (L\sin\alpha_d - L, L\sin\alpha_d + L). \tag{10}$$

At the boundaries of this interval, the two values of q_{1d} collapse into a single solution. Not surprisingly, the existence of a solution depends on a relation between the desired orientation α_d and the y-position p_{yd} of the end-effector. For instance, if $\alpha_d = \pi/2$, then (at least) a solution exists for $p_{yd} \in [0, 2L]$; if $\alpha_d = -\pi/2$, a solution exists for $p_{yd} \in [-2L, 0]$. The value of p_{xd} plays no role in this analysis, as long as there is no limit to the range of the prismatic joint q_1 (see also the

[1] For $q_3 \in (0, \pi)$, M_z is positive (counterclockwise) and the torque at joint 3 produced by F_y is negative (clockwise).

following workspace analysis). For each solution q_{1d} in (9), consider again the first two equations in (1) and, by using (8), solve for q_2 as

$$q_{2d} = \text{ATAN2}\left\{\frac{p_{yd}}{L} - \sin\alpha_d, \frac{p_{xd} - q_{1d}}{L} - \cos\alpha_d\right\}. \tag{11}$$

Finally,

$$q_{3d} = \alpha_d - q_{2d}. \tag{12}$$

Therefore, (at most) two solutions $\boldsymbol{q}_d$ are found in closed form by using eqs. (9), (11) and (12). Evaluating the inverse kinematics with the data $L = 0.5$ and $\boldsymbol{r}_d = (0.3, 0.7, \pi/3)$ provides the two regular solutions

$$\boldsymbol{q}_d^{(i)} = \begin{pmatrix} q_{1d}^{(i)} \\ q_{2d}^{(i)} \\ q_{3d}^{(i)} \end{pmatrix} = \begin{pmatrix} 0.4728 \\ 2.5783 \\ -1.5311 \end{pmatrix} \quad \text{and} \quad \boldsymbol{q}_d^{(ii)} = \begin{pmatrix} q_{1d}^{(ii)} \\ q_{2d}^{(ii)} \\ q_{3d}^{(ii)} \end{pmatrix} = \begin{pmatrix} -0.3728 \\ 0.5633 \\ 0.4839 \end{pmatrix} \text{ [m,rad,rad].}$$

At last, Fig. 2 shows the primary and secondary workspaces for this robot, taking into account the finite range $q_1 \in [0, L]$ of the prismatic joint. As usual, the primary workspace WS_1 is the set of points in $\mathbb{R}^2$ that can be reached with at least one of the admissible orientations (in the plane) of the robot end effector. A point $P \in WS_1$ belongs also to the secondary workspace WS_2 if it can be reached with *all* the admissible orientations of the end effector. In the present case, this happens only for points on the (green) segment OD in Fig. 2. If there were no bounds on the range of q_1, both WS_1 and WS_2 would expand limitless along the positive and negative $\boldsymbol{x}_0$ direction (WS_1 would be an infinite horizontal stripe of height $4L$).

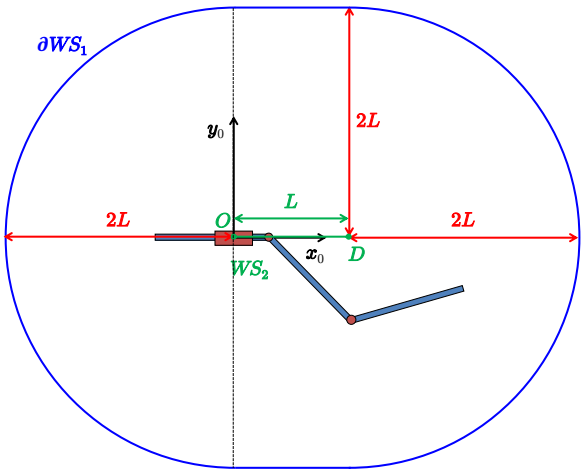

Figure 2: The primary workspace WS_1 (with boundary ∂WS_1 in blue) and the secondary workspace WS_2 (the line from O to D in green) of the PRR robot in Fig. 1.

A remark is in order on the relation between the definition of the above robot workspaces and the number of solutions to the inverse kinematics of the considered task. Although in general these are two different problems (e.g., the task of a robot may or may not involve the end-effector orientation), few simple observations can be made in the present setting:

- outside WS_1 there is no solution for the task $\boldsymbol{r} = \boldsymbol{r}_d$;

- on the boundary ∂WS_1, there is at most a single solution to the task (this happens when the desired orientation α_d takes a single special value at each $\boldsymbol{p}_d \in \partial WS_1$);
- in the interior $\overline{WS}_1$, there are at most two solutions to the task, depending on the satisfaction of the relation (10) between p_{yd} and α_d;
- when $\boldsymbol{p}_d \in WS_2$, there is always at least a solution to the task, for any value of α_d;
- in any case, solutions may be discarded by the presence of a limited range for the prismatic joint (i.e., if $q_{1d} \notin [0, L]$, as computed by eq. (9)), as well as by finite ranges of the revolute joints.

Exercise #2

This trajectory planning problem in the joint space of the PRR robot takes advantage of the availability of a closed form solution for the inverse task kinematics, as obtained in Exercise #1, but it is also greatly simplified by the particular symmetry of the data in the given problem. With reference to Fig. 3, we shall plan first a smooth trajectory for $\alpha_d(t)$ which, according to (8), will also be the trajectory for the sum of the two joint angles $q_{2d}(t) + q_{3d}(t)$. However, by the symmetries of the task, $q_{2d}(t) = -\alpha_d(t)$ and so $q_{3d}(t) = 2\alpha_d(t)$. Since the robot end effector point P has to remain at rest in the constant position $\boldsymbol{p}_d = \boldsymbol{p}_i = \boldsymbol{p}_f$, for all $t \in [0, T]$, the tip position $\boldsymbol{p}_2$ of the second link will trace an arc of a circle (with an absolute speed equal to $|\dot{\alpha}_d(t)|$). Taking into account the obtained trajectory $q_{2d}(t)$, this motion is realized by an oscillatory motion of $q_{1d}(t)$ that will move the base of link 2 accordingly. Note that all joint trajectories will behave symmetrically w.r.t. to the midtime $T/2$. Obviously, the same behavior is obtained from the closed-form solution of the inverse task kinematics in Exercise #1, but the previous analysis is simpler and does not presume the availability of such expressions.

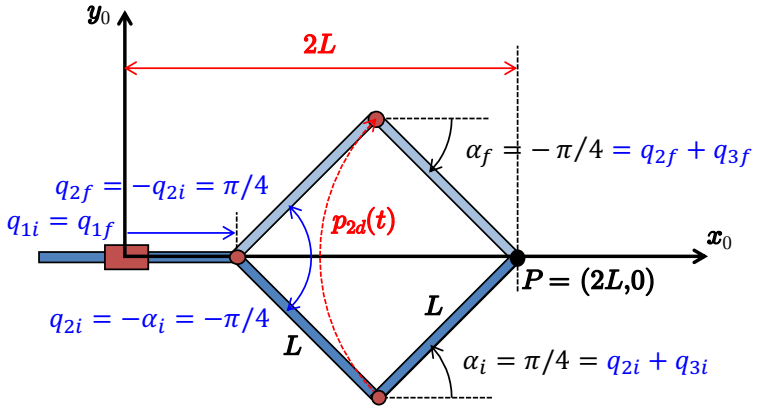

Figure 3: The given trajectory planning problem has symmetries in space (in particular, w.r.t. the axis $\boldsymbol{x}_0$) and in time.

With the above in mind, we plan a cubic[2] rest-to-rest trajectory for α:

$$\alpha_d(t) = \alpha_i + (\alpha_f - \alpha_i)\left(3\left(\frac{t}{T}\right)^2 - 2\left(\frac{t}{T}\right)^3\right), \qquad t \in [0, T],$$

with

$$\dot{\alpha}_d(t) = \frac{\alpha_f - \alpha_i}{T}\left(6\left(\frac{t}{T}\right) - 6\left(\frac{t}{T}\right)^2\right), \qquad \ddot{\alpha}_d(t) = \frac{\alpha_f - \alpha_i}{T^2}\left(6 - 12\left(\frac{t}{T}\right)\right).$$

[2]Also a quintic polynomial could have been used, wishing to start and end the motion with zero acceleration.

Substituting the initial and final values for α, we have

$$\alpha_d(t) = \frac{\pi}{4} - \frac{\pi}{2}\left(3\left(\frac{t}{T}\right)^2 - 2\left(\frac{t}{T}\right)^3\right), \qquad t \in [0, T],$$

The desired trajectory of the tip of the second link is

$$\boldsymbol{p}_{2d}(t) = \boldsymbol{p}_d - L\begin{pmatrix}\cos\alpha_d(t)\\ \sin\alpha_d(t)\end{pmatrix} = \begin{pmatrix}2L\\ 0\end{pmatrix} - L\begin{pmatrix}\cos\alpha_d(t)\\ \sin\alpha_d(t)\end{pmatrix}, \qquad t \in [0, T].$$

Taking advantage of the symmetries, we obtain then

$$\begin{aligned} q_{2d}(t) &= -\alpha_d(t),\\ q_{3d}(t) &= \alpha_d(t) - q_{2d}(t) = 2\alpha_d(t), \qquad t \in [0, T].\\ q_{1d}(t) &= p_{xd} - L\left(\cos\alpha_d(t) + \cos q_{2d}(t)\right) = 2L\left(1 - \cos\alpha_d(t)\right), \end{aligned} \tag{13}$$

Figure 4 shows the evolution in normalized time $\tau = t/T \in [0, 1]$ of the components of the planned joint trajectory $\boldsymbol{q}_d(\tau)$ obtained by (13) and of those of the resulting task trajectory $\boldsymbol{r}_d(\tau)$, as computed by the direct kinematics (1). For these plots, a link length $L = 0.5$ [m] has been chosen. Note that p_{xd} and p_{yd} remain constant at their initial value, as desired.

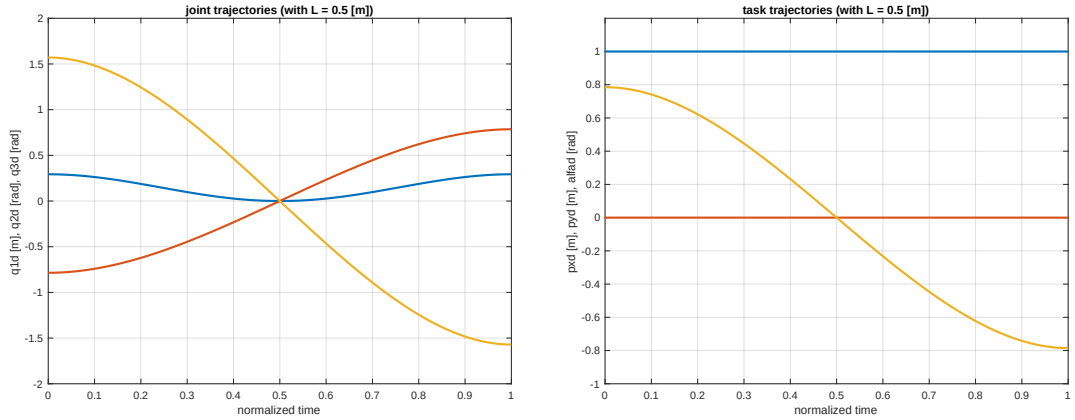

Figure 4: Joint trajectory $\boldsymbol{q}_d(\tau) = (q_{1d}(\tau), q_{2d}(\tau), q_{3d}(\tau))$ [blue, red, yellow] from (13) and associated task trajectory $\boldsymbol{r}_d(\tau) = (p_{xd}(\tau), p_{yd}(\tau), \alpha_d(\tau))$ [blue, red, yellow] in normalized time.

For comparison, use the given data in the closed-form expressions (9), (11) and (12) of the inverse task kinematics. These yield:

$$\begin{aligned} q_{1d}(t) &= 2L - L\cos\alpha_d \pm \sqrt{L^2\cos^2\alpha_d} = \begin{cases} 2L\\ 2L\left(1 - \cos\alpha_d(t)\right), \end{cases}\\ q_{2d}(t) &= \mathrm{ATAN2}\left\{-\sin\alpha_d(t), \frac{2L - q_{1d}(t)}{L} - \cos\alpha_d(t)\right\}\\ &= \mathrm{ATAN2}\left\{-\sin\alpha_d(t), \mp\cos\alpha_d(t)\right\} = \begin{cases} \alpha_d(t) - \pi\\ -\alpha_d(t), \end{cases}\\ q_{3d}(t) &= \alpha_d(t) - q_{2d}(t) = \begin{cases} \pi\\ 2\alpha_d(t), \end{cases} \end{aligned} \qquad t \in [0, T]. \tag{14}$$

It is apparent that a second, alternative solution is available: the first joint remains at rest, placing the base of the second link in P; the second joint rotates as $\alpha_d(t)$, modulo an angular displacement of $-\pi$; the third joint is also fixed, with the third link folded on the second, so that the position of the robot end effector is always constant and equal to $\boldsymbol{p}_d$. Figure 5 shows the results when using for $\boldsymbol{q}_d(\tau)$ the alternative solution in (14) (and again, with $L = 0.5$ [m]). Indeed, the resulting task trajectory $\boldsymbol{r}_d(\tau)$ is the same.

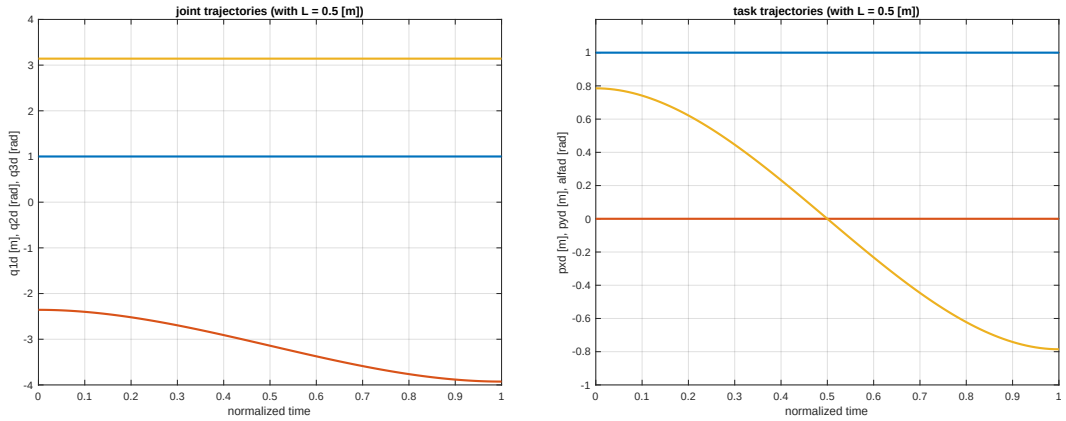

Figure 5: Alternative joint trajectory $\boldsymbol{q}_d(\tau) = (q_{1d}(\tau), q_{2d}(\tau), q_{3d}(\tau))$ [blue, red, yellow] from (14) and associated task trajectory $\boldsymbol{r}_d(\tau) = (p_{xd}(\tau), p_{yd}(\tau), \alpha_d(\tau))$ [blue, red, yellow] in normalized time.

* * * * *